

## A new model for predicting the effective strength in reinforced concrete bottle-shaped struts

A. Arabzadeh<sup>1,\*</sup>, R. Aghayari<sup>2</sup>, A. R. Rahai<sup>3</sup>

Received: October 2010, Revised: January 2012, Accepted: May 2012

### Abstract

*Strut-and-Tie Model (STM) can be used to model the flow of compression within a concrete strut. Concrete struts are formed in various shapes such as prismatic or bottle-shaped. In order to study the behavior of concrete struts, a series of simple tests were performed. Eighteen reinforced concrete isolated struts with compressive strength of 65 MPa were tested up failure under point loading in the plane of specimens. The tested specimens were reinforced by various reinforcement layouts. The behavior of tested beams was investigated. Observations were made on transverse displacement, primary cracking and ultimate failure load and distribution of strain on the face of tested panels. Based on these observations, the geometry of the concrete struts was examined. A new model to analysis of concrete struts was proposed based on modified compression field theory (MCFT). A database of 44 tested specimens was compiled to evaluate the proposed model. The results indicate that using the ACI and CSA codes expressions regarding the amount of minimum required reinforcement in a strut produces conservative but erratic results when compared with the test data. Conversely, the new proposed model presents a more accurate prediction for the strength of 44 tested struts.*

**Keywords:** *Strut-and-tie, Transverse reinforcement, Strut, Efficiency factor.*

### 1. Introduction

Strut-and-tie method (STM) is one of the most simple and applicable methods that can be used to reduce complex states of stresses within concrete structures to a collection of simple stress paths. The base of STM was laid by Ritter (1899) [1]. Ritter's original goal was to explain a stirrup in RC members, Ritter's model was expanded later by Mörsch (1902); Mörsch presented that the diagonal compressive stresses in the concrete would not to be discrete zones, but could be continuous field in equilibrium with discrete stirrup forces [2]. The Strut-and-Tie Method (STM) is gaining rapid popularity for shear RC members such as corbels, deep beams and beam-column joints. Marti (1986) [3], Schlaich-Schäfer, (1987) [4], Mitchell-Collins (1984) [5], Rameriz (1994) [6], Tang et al (2001) [7] and Hwang et al (2002) [8] proposed some

approaches applicable in D-regions. Author et al proposed a new method based on Strut-and-Tie Model (STM) to determine the shear capacity of simply supported RC deep beams and an efficiency factor for concrete with considering the effect of web reinforcements [9].

Struts as important element of strut-and-tie model carry compressive forces and their forming shapes varies depend on the force path. The most basic type of struts is prismatic with uniform cross-section over its length. The compressive stress block in the pure-bending region of deep beams can be an example of prismatic strut [10]. When the flow of compression stress is not confined to a portion of structural element, a bottle-shape strut forms that the force is applied to a small zone and disperses as they flow through the member. Its bulging stress paths cause the significant transverse strain perpendicular to strut axis. The formed transverse strain is compressive in near of both neck of bottle-shape strut and tensile further away [4]. Consequently, those strains cause longitudinal cracks and initiate an early failure. It is therefore necessary to reinforce the stress field in transverse direction or to consider the transverse tension to predict the ultimate strength of strut.

Some studies have been published to investigate the behavior of RC bottle-shape struts and establish their ultimate strength on the basis of mechanic-based models. Brown et al

\* Corresponding Author: arabzade@modares.ac.ir  
1 Associate Professor, Structural Engineering Dept., Tarbiat Modarres University, Tehran, Iran  
2 Assistant Professor, Civil Engineering Dept., Razi University, Kermanshah, Iran  
3 Professor, Faculty of Civil Engineering, Amir Kabir University of Technology, Iran

(2006) [10], [11] published two papers that investigated the behavior of normal-strength concrete isolated struts and minimum requirement transverse reinforcement.

The dispersion of compression was described in great detail by Guyon (1953). Guyon used flow paths to determine the dispersion of tensile and compressive stresses in a post-tension zone and concluded that the flow paths of compression (1 through 6 in Fig.1) must be parallel to the applied force at loaded point and some distance away from it [10].

The resulted tensile force forms perpendicular to the compression curve paths. It means that, the bottle-shape struts can be modeled as a combination of accessory struts and ties as shown in Fig.2.

In this paper, the efficiency factors presented in ACI 318-08 and CSA codes are investigated. In addition, a new relation based on modified compression field theory (MCFT) is proposed. To evaluate of proposed model, the ultimate capacity of 44 tested isolated concrete struts were determined and compared with the results of the CSA [12] and ACI 318-08 [13] approaches.

## 2. Geometry of bottle-shaped struts

A bottle-shaped strut can be modeled by a collection of struts and ties as presented in Fig.2 this model composed of transverse ties, diagonal and longitudinal struts. The dispersion of compression indicates the inclination angle of diagonal strut.

According to ACI 318-08 [13] provisions, the compressive force flows by dispersion slope of 1:2 (two unit along longitudinal axis and one unit transverse that axis). For this model no recommendation is provided to the placement of

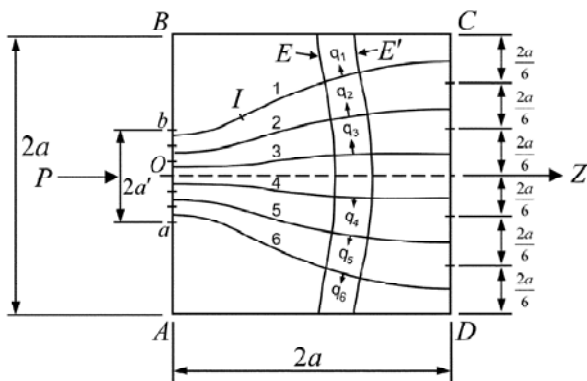


Fig. 1 Dispersion of compression provided by Guyon [10]

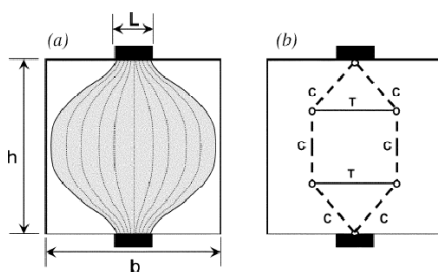


Fig. 2 The actual and simplified forms of bottle-shaped strut [10]

formed ties. Therefore, three various shape of bottle-shaped can be formed in concrete struts. According to Saint Venant's principle, when the width of strut is larger than two times of its overall depth, the strut forms in diamond-shape (Fig.3.a). Otherwise the cases "b" and "c" are the usual shapes of struts, "c" form occurs in long concrete struts such as columns.

Schalich and Weishede [14] suggested a combined STM for modeling of bottle-shape strut which within it the compressive force disperses with a slope dependent on the width of bottle neck and length of strut (Fig.4). It is defined by:

$$m = \frac{2b_f}{b_{ef} - b_{min}} \quad (1)$$

$$\begin{aligned} b_{ef} &= L/3 & (b_{min} < L/3) \\ b_{ef} &= L/6 + b_{min} & (b_{min} \geq L/3) \end{aligned} \quad (2)$$

Where,  $b_{min}$  the width of strut neck,  $b_{ef}$  the effective width of strut,  $L$  the length of strut and  $m$  is the slope of stress dispersion.

Fig. 5 shows a strut-and-tie model includes a constant slope for dispersion of compression as "m". According to equilibrium of this model, the transverse component of dispread force is carried by transverse ties, it can be written as:

$$F_D/2 = C \cos \theta \quad (3)$$

$$F = 2C \sin \theta \quad (4)$$

$$T = F / \tan \theta = F/m \quad (5)$$

Where  $F$  is the applied load,  $F_D$  is total transverse force;  $C$  is the compressive force of inclined struts and  $\theta$  is the angle of dispersion of compression or strut inclination.

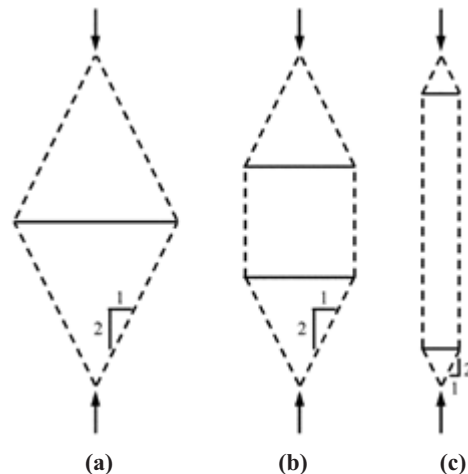


Fig. 3 Various shapes of bottle-shaped strut. [11]

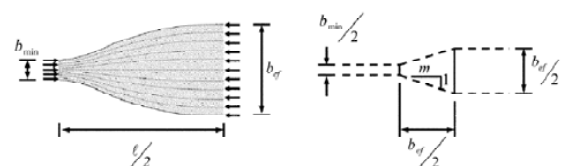


Fig. 4 bottle-shape model provided by Schalich – Weishede [14]

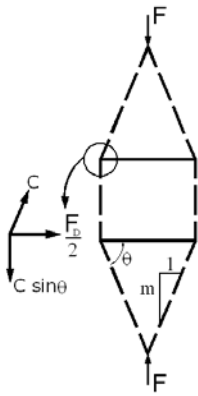


Fig. 5 equilibrium of simplified bottle-shaped strut

### 3. Testing program

#### 3.1. specimens detail

Test specimens consisted of eighteen concrete plain panels that measured 400×400×60 mm and were loaded using steel bearing plates that were 120×60×12 mm defining the nodal zone. The concrete was prepared by Type II Portland Cement and river fine aggregate. Maximum aggregate size was 9.5 mm (3/8 inch) and the slump was approximately 90 mm. The concrete strength was defined 65 MPa based on the average value of three standard cylinders (300×150 mm). The primary variables were the amount and placement of the reinforcing bars. The specimens were classified in the following series based on the various patterns of used transverse reinforcement.

i. Series A, in this series, the reinforcement was either uniformly distributed or concentrated at locations that

correspond to the discrete ties in the STM

ii. Series B, this series of specimens was reinforced with uniformly distributed transverse reinforcement.

iii. Series C, in the third series of specimens, the transverse reinforcement was concentrated at near of top and bottom nodal zone with uniform spacing against to series A.

iv. Specimens D-1 which was reinforced in two orthogonal directions by uniform spacing, E-1 with transverse reinforcement same as A-2 and added longitudinal steel bars placed under the loading surface, F-1 with inclined orthogonal reinforcement and H-1 consisted of no reinforcement.

Each of the specimens is described in detail of Fig.6; the tested panels were employed supplemental confinement at the nodal zones. This confinement consisted of short pieces of reinforcing 6D (6mm-dia.) bars welded to a steel plate and surrounded by ties bent from 6D (6mm-dia.) bars (Fig.7).

#### 3.2. Steel bars properties

Used steel bars consisted of 8D (8mm-dia.) and 6D (6mm-dia.). All specimens were reinforced by 8D bars except for B-1 which was reinforced by 6D bars. Table 1 shows further details of mechanical properties obtained from tensile test of steel bars.

#### 3.3. Testing setup

The test setup was similar to split-cylinder testing by a monotonic load with an increasing rate applied at top face of specimen trough bearing steel plate. The basic setup of test is shown in fig.8, Strain measurements were performed via series of electric strain gauges attached to the concrete surface of the specimens. The measured strains were recorded through data-

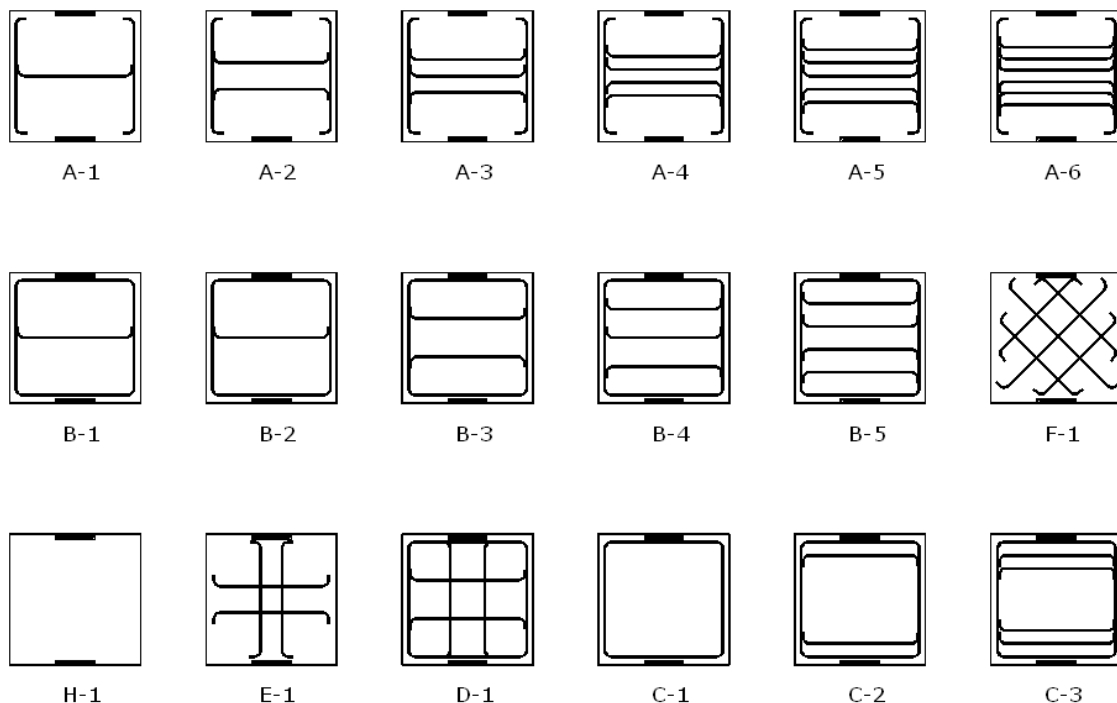


Fig. 6 Detail of specimens

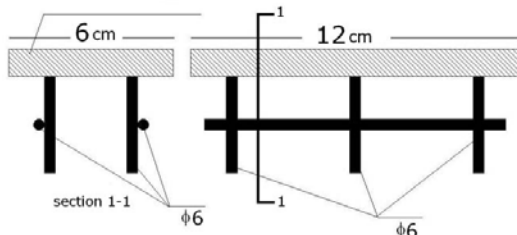


Fig. 7 Used detail in nodal zone

Table 1 Mechanical properties of used steel bars

Bar ID.	$\epsilon_y$	$\epsilon_u$	$f_y$ (MPa)	$f_u$ (MPa)	E (MPa)
8D	0.207%	11.2%	416	487	201000
6D	0.192%	9.70%	397	469	207200

logger hardware. To report and record the magnitude of applied load, a load cell placed between the hydraulic jack and the strong girder of reaction frame

## 4. Experimental observations

### 4.1. General behavior of struts

All specimens presented a same behavior. As in initial steps of loading a vertical crack was formed approximately at the mid-height of the specimens. By increasing the applied load, this crack propagated toward the top and bottom loaded edges. As the crack reached near to top or bottom loading surface, it changed direction and curved toward out of loaded zone (Fig.9.a). However the ultimate failure occurred due to extreme splitting of concrete at mid-height of tested strut. In The over-reinforced specimens, ultimate failure was initiated by crushing of the concrete near, but not adjacent to the loading points (Fig.9.b).

Table 2 presents the cracking and ultimate failure load obtained from tests. To calculate the efficiency factor  $\eta$  on the basis of experimental data, the applied load at failure of the specimen was divided by the bearing area of that particular specimen times the compressive strength.

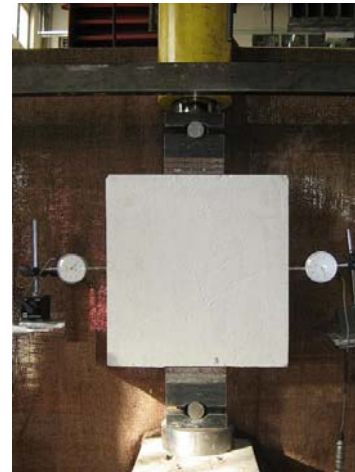
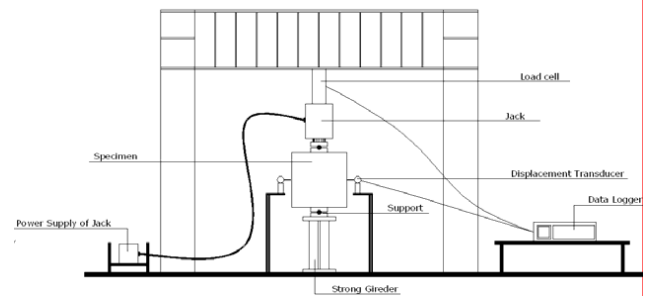


Fig. 8 Testing setup

### 4.2. Geometry of formed bottle-shape struts

In regard to the formation and propagation of vertical cracks in initial stages of loading, this implies that the maximum tensile strains occurred at the mid-height of specimen. Therefore on the basis of the stress dispersion model proposed by Guyon, the adequate presentation force system within the tested struts is the diamond-scheme (Fig.10). This STM consisted of four diagonal struts with no vertical strut. However, it can be pointed out that for the full development of Guyon's stress trajectories, the STM is formed in fully bottle-shape with two vertical struts when the length of strut is at least twice the maximum width of strut.



a. Crack forming



b. Crushing of nodal zone

Fig. 9 general behavior of tested specimens



**Table 2** Experimental results

Specimen ID	Ultimate Load $V_u$ (kN)	Cracking Load $V_{cr}$ (kN)	$\nu^*$	$\frac{V_u}{V_{cr}}$
A-1	258	205	0.55	0.79
A-2	371	271	0.79	0.73
A-3	432	307	0.92	0.71
A-4	465	330	0.99	0.71
A-5	479	325	1.02	0.69
A-6	481	325	1.04	0.66
B-1	221	172	0.47	0.78
B-2	343	257	0.73	0.75
B-3	418	288	0.89	0.69
B-4	461	323	0.98	0.70
B-5	465	293	0.99	0.65
C-1	268	155	0.57	0.58
C-2	343	170	0.73	0.49
C-3	423	260	0.90	0.61
D-1	401	230	0.87	0.57
E-1	381	243	0.81	0.64
F-1	353	215	0.75	0.61
H-1	184	137	0.39	0.74

$$\nu^* = \frac{\text{Ultimate Load}}{f'_c \times \text{Bearing Area}}$$

#### 4.3. Effect of transverse reinforcement

It is clear from the observation of the failure mechanism of tested struts that, In each group, there is a considerable variation in the experimental strength, as the amount of transverse reinforcement increased, the ultimate capacity of specimens increases and the failure mode changed from a tensile failure of concrete away from the crushing of concrete at or near the loaded edges.

The marked increase in percentage of transverse reinforcement was not associated with significant increase in ultimate strength of over-reinforced specimens than under-specimens. It means that, by satisfying the requirement reinforcement the bottle-shaped strut can be able to maintain equilibrium and additional transverse reinforcement only controls the width of cracks and cannot prevent tensile failure, In other word, to improve the strength of softened concrete, only an intermediate amount of transverse reinforcement can be sufficient to maintain equilibrium in the bottle-shaped STM, additional reinforcement may be necessary for the purposes of serviceability.

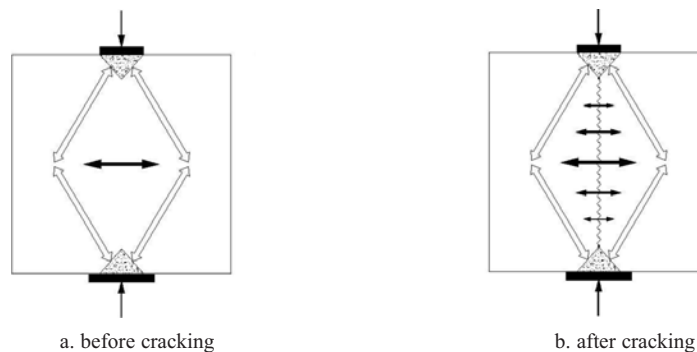


**Fig. 11** Typical STM at various loading stages

#### 4.4. Effect of transverse reinforcement arrangement

The ultimate capacity of specimens contained reinforcement lumped at the middle region of strut was measured greater than other specimens with same amount of transverse reinforcement. Because of high transverse tensile straining at the center of struts, it is logical that, the concentration of reinforcement at this region can resist the occurred tensile stresses and be more effective compared with specimens despite the presence of reinforcement that was distributed by uniform spacing. In addition, lumping of transverse reinforcement near to the loading surfaces decreases the efficiency of transverse reinforcement, as the experimental capacity of specimens in series C was less in comparison with those in series A and B that were reinforced with same percentage of reinforcement (Fig.10).

It is concluded that from experimental observations, once the initial crack appears, the concrete stiffness reduces significantly. By increasing the applied load, the system of STM was changed and the vertical crack propagates toward loading surfaces of strut (Fig.11). At least before ultimate failure of strut a series of secondary-ties appears with slight level of stress due to redistribution of middle tensile stresses. The arrangement of transverse reinforcement is one of the efficient parameters on ultimate capacity of RC struts [15].

#### 4.5. The system of stress Dispersion

In order to investigate the system of stress dispersion and the geometry of STM in tested specimens, 13 strain gages were placed across the width of some specimens such as H-1, A-4, B-

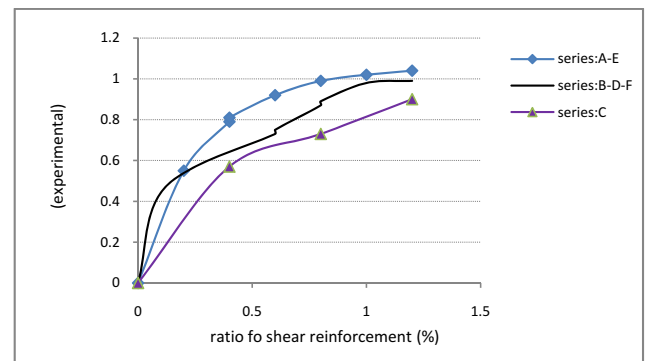


**Fig. 10** Comparison the efficiency of shear reinforcement

2, D-1 and C-2. The marked gages were oriented vertically and were distributed at regular interval along the center axis of strut. Beyond the cracking the recorded results from gages crossed the major vertical crack were not usable because of extreme strains; therefore the measured strains were investigated for elastic distribution of stress before formation of cracks. To obtain the stresses of concrete at various load stages, the records of strain were converted to stresses using the elastic-plastic relationship resulted from pressure test of standard-cylinders.

The strain distribution of Specimens is shown in Fig.12 given that the test data:

- i. Across the width of strut, stress reduces with receding from panel centerline.
- ii. Along the centerline of panels, strain increases with receding from strut center

Based on the shown in Fig.12 that presents the distribution of compressive stress in H-1 specimen, approximately a

symmetric stress distribution was observed across the width of strut as the major impact of stress occurred under the loading plate.

In Fig.13 a composite of stress distributions for marked specimens. At least, resulting from further analysis, the angle of dispersion was estimated to have a slope of 3:1 ( $m = 3$  in Figure 5) which differs from that provided by ACI 318-08 [13].

### 5. Resulted resistant tensile force in the transverse reinforcement

The main role of transverse reinforcement is controlling the crack development and preventing the excessive opening of them. Because of transverse tensile straining the initial cracks are formed in the longitudinal direction. It means that the transverse reinforcement is most effective when used perpendicular to the loading direction.

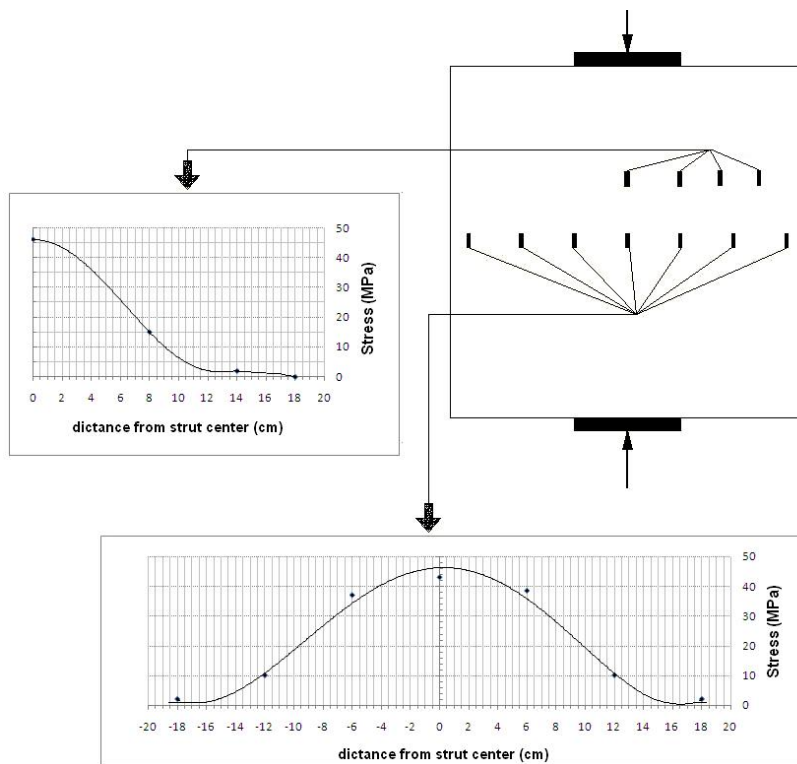


Fig. 12 Stress dispersion of B-2 specimen

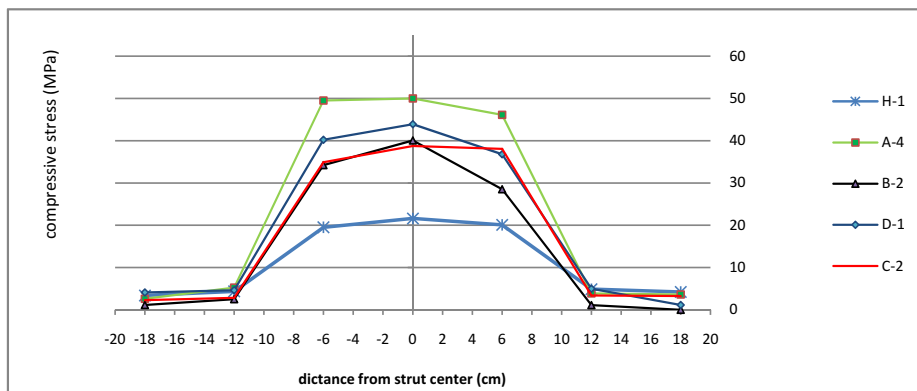


Fig. 13 Comparison of stress dispersion of specimens

On the basis of experimental results, the requirement amount of transverse reinforcement depends on concrete strength. The role of transverse reinforcement is very important and sensitive as high-strength concrete exhibits more brittle and abrupt failure than normal-strength concrete. As shown in Fig.14, if the fully cracked strut without any shear slip is assumed along the crack, all transverse tensile straining are resisted by reinforcing bars beyond the forming of initial cracks. By assuming the yielding of transverse reinforcement once the concrete splits, it can be resulted:

$$F_D = F_u + F_v = A_u f_{yu} \sin\theta + A_v f_{yv} \cos\theta \quad (6)$$

Where,  $f_{yu}$  and  $f_{yv}$  are the tensile yield stresses of bars in  $u$  and  $v$  directions respectively,  $A_u$  and  $A_v$  the area of bars in  $u$  and  $v$  directions respectively,  $\theta$  is the angle between  $u$  direction and strut axis,  $F_D$  the yield force of transverse reinforcement. If the used reinforcement is equalized to  $A_w$ , it can be written as:

$$F_D = A_w f_y = \rho_D (L_s b_s) f_y \quad (7)$$

Where  $\rho_D$  means the ratio of equivalent reinforcement that defined as:  $\rho_D = A_w / (b_s L_s)$ ,  $b_s$  and  $L_s$  are the width and length of strut. By substituting the  $f_y = f_{yu} = f_{yv}$  in Eq. 6 and comparison of Eq.7 and Eq.6, it can be written:

$$\rho_D = \frac{A_u}{L_s b_s} \sin\theta + \frac{A_v}{L_s b_s} \cos\theta \quad (8)$$

According to ( $a = L_s \cos\theta$ ) and ( $d = L_s \sin\theta$ ),  $\rho_D$  can be calculated as:

$$\rho_D = \frac{A_u}{b_s d} \sin^2\theta + \frac{A_v}{b_s d} \cos^2\theta \quad (9)$$

or:

$$\rho_D = \rho_u \sin^2\theta + \rho_v \cos^2\theta \quad (10)$$

$\rho_u$ ,  $\rho_v$  are the ratios of reinforcement in  $u$  and  $v$  directions respectively.

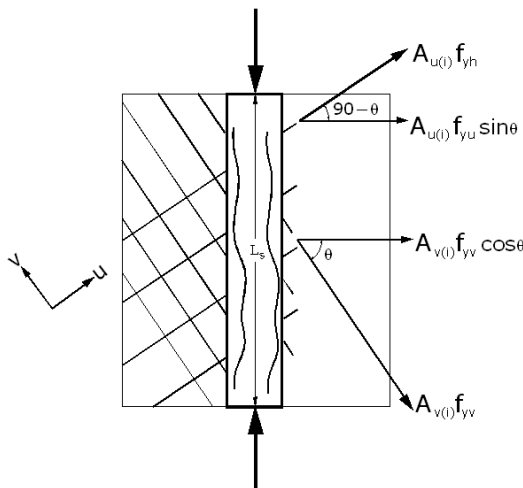


Fig. 14 Resulted tensile force due to transverse reinforcement

## 6. ACI 318-08 provisions to predict the effective strength of concrete

According to recommendations of ACI 318-08 [13], struts are classified to five categories according to that, the efficiency factor of concrete strength  $\beta_s$  is obtained based on satisfying the minimum requirement amount provided in A.3.3 section of ACI 318-08 [13]. By means of, as concrete strength is greater than 40 MPa, the minimum necessary transverse reinforcement to avoid of concrete splitting is estimated by assuming the slope of 1:2 for dispersion of compression and yielding of reinforcement. If sufficient transverse reinforcement exists within concrete strut, the larger  $\beta_s$  factor of 0.75 is used, otherwise  $\beta_s$  must be assumed as 0.6, The minimum requirement reinforcement from section A.3.3 of ACI 318-08 is provided to resist the total transverse tension [13]. The amount of confining transverse reinforcement can be computed using the strut-and-tie model shown in Fig. 5 with the struts that represent the spread of the compression force acting at a slope of 1:2 to the axis of the applied compressive force. Alternatively for specified concrete compressive strengths not exceeding 40 MPa, the amount of reinforcement required by Eq.11 is deemed to satisfy section A.3.3 of ACI 318-08

$$\sum \frac{A_{si}}{b_s i} \sin\alpha_i \geq 0.003 \quad (11)$$

Where,  $A_{si}$ ,  $S_i$ ,  $\alpha_i$  are the area, spacing and the angle between axis of strut and bars in  $i$ -th layer of reinforcement crossing that strut. and  $b$  is the width of strut, if the reinforcement is used with constant spacing Eq. 11 can be derived to:

$$\rho_D = \rho_u \sin\theta + \rho_v \cos\theta \geq 0.003 \quad (12)$$

In addition, for deep beams which will likely contain bottle-shaped struts, in chapter 11 of ACI 318-08 [13] the additional minimum shear reinforcement ratios of 0.25% and 0.15% are provided in vertical and horizontal directions, respectively. But according to section 11.7.6 it shall be permitted to provide reinforcement satisfying A.3.3 instead of that horizontal and vertical minimum reinforcement. It means that the designer is allowed to eliminate the transverse reinforcement if the lower efficiency factor of concrete strength ( $\nu=0.6$ ) is used.

Based on the provisions of A.3.3 section, by assuming the slope of dispersion of compression equals to 2, the minimum requirement transverse reinforcement of bottle-shape struts can be computed as:

$$\rho_D = \frac{P_u}{2f_y b L_s} \quad (13)$$

where,  $\rho_u$  is the applied load,  $b$  is the width of beam,  $L_s$  the length of strut and  $f_y$  is the tensile yield stress of steel bars.

## 7. The approach of CSA

The Canadian standard CSA [12] defines the efficiency strength of concrete on the basis of Modified Compression

Field Theory (MCFT) as follows:

$$f_{cu} = \frac{f'_c}{0.8+170\varepsilon_1} \leq 0.85 f'_c \quad (14)$$

$$\varepsilon_1 = \varepsilon_s + (0.002) \cot^2 \alpha_s \quad (15)$$

Where  $f_{cu}$  the efficiency strength of concrete,  $\alpha_s$  the angle between strut and tie,  $\varepsilon_s$  the tensile strain of cracked concrete and  $f'_c$  is the specified concrete strength.

As seen that, rather than using the amount of transverse reinforcement as in ACI 318-08, CSA bases the efficiency concrete strength on an average strain in the concrete at the location of ties. In applying the design form of MCFT as provided in CSA, many designing engineers have had difficulty in substituting an adequate amount of  $\varepsilon_s$ . If the strain term is eliminated, the provisions of CSA would be likely more useful for practicing designers.

## 8. The new model for prediction of efficiency factor based on MCFT

In the nonlinear finite elements analysis of reinforced concrete structures it is necessary to use constitutive model for concrete that are based on smeared-rotating crack idealization. Moreover, cracked reinforced concrete in compression has been observed to exhibit lower strength and stiffness than uniaxially-compressed concrete. This degradation is primarily related to the degree of transverse straining and cracking present in the concrete. Many of analytical models for describing the softening effect were derived from experimental data and proposed in rational or semi-rational form. Vecchio et al [16] presented the compressive softening of concrete as fig.15,  $v$  is the efficiency factor of concrete strength and can be determined by:

$$v = \frac{1}{1+K_c K_f} \quad (17)$$

$$K_c = 0.27 \left( \frac{\varepsilon_1}{\varepsilon_0} - 0.37 \right) \quad (18)$$

$$K_f = 0.1825 \sqrt{f'_c} \quad (19)$$

Where,  $\varepsilon_1$ ,  $\varepsilon_0$  are the average principal tensile strain and the strain at the peak cylinder stress and  $f'_c$  is the specified strength of concrete. Controlling the width of cracks is an important role of transverse reinforcement. According to experimental observations while the cracks of concrete are forming, the

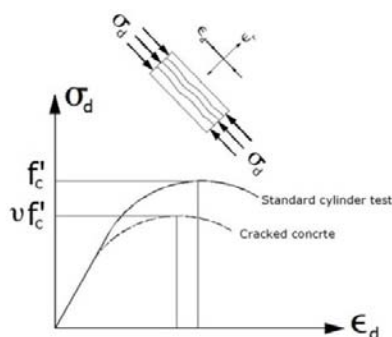


Fig.15 Compression softening of cracked concrete

transverse reinforcing bars are subjected to tensile strain and prevent to cracks opening. In strut-and-tie modeling the cracking of concrete is assumed fully without any shear slip and therefore, it can be implies that the occurred transverse tensile force are resisted by transverse reinforcement, by assuming no shear force, the principal tensile strain can be computed as:

$$\varepsilon_1 = \frac{T}{EA_w} \quad (20)$$

Where  $T$  is transverse tensile force,  $E$  is the module of elasticity and  $A_w$  is the area of equivalent transverse reinforcement obtained by:

$$A_w = \rho_D b L_s \quad (21)$$

where  $\rho_D$  is the ratio of equivalent transverse reinforcement,  $b$  the width of strut and  $L_s$  is the length of strut.

As presented in eq.5, the total occurred transverse tensile force can be determined by:

$$T = \frac{P}{m} = \frac{v A_{str} f'_c}{m} \quad (22)$$

Where,  $v$  is the efficiency factor of concrete strength,  $f'_c$  is the specified strength of concrete and  $A_{str}$  is the cross-sectional area of strut. By substituting of  $m=3$  as was estimated in current study and simplifying Equations. 16 through 21, following equations are resulted for prediction of  $v$  :

$$0.27 K_f K_v^2 + (1 - (0.37 + \cot^2 \theta)) K_f v - 1 = 0 \quad (23)$$

$$K = \frac{f'_c w}{3E \rho_D L_s \varepsilon_2} (1 + \cot^2 \theta) \quad (24)$$

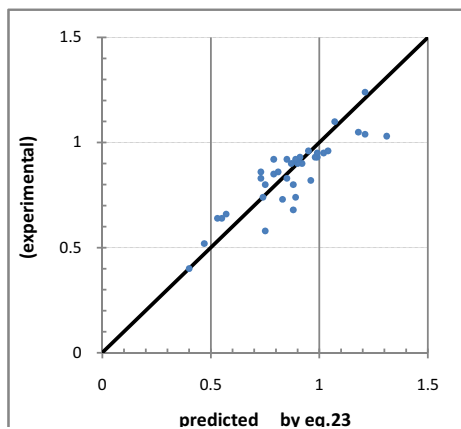
By assuming the  $\varepsilon_2=0.003$  and  $E=200000$  MPa, Eq.23 is simplified to

$$K = \frac{f'_c w}{1800 \rho_D L_s} (1 + \cot^2 \theta) \quad (25)$$

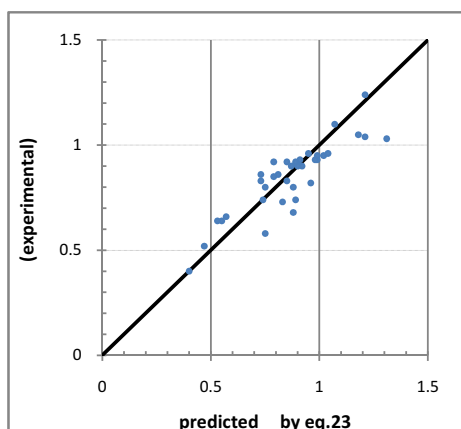
where,  $w$  is the width of loaded plate or minimum width of bottle-shaped strut. A database consisted of eighteen concrete panels tested by author et al and twenty six concrete panels tested by brown et al [11] was used to evaluate the proposed equation. The ultimate capacity of selected specimens were determined and compared with experimental data and results of both approaches of CSA [12] and ACI 318-08 [13]. Fig.16 shows a correlation between measured efficiency factor of concrete strength and predicted value by provisions of both codes. As presented, the provided method by ACI 318-08 is more scattered than provision of CSA. In addition, the results of new proposed model have the best agreement with experimental data. According to performed investigation, it can be concluded that:

a. The ACI 318-08 provisions predicted more scattered results than CSA and new proposed model. The predicted efficiency factor is unsafe for specified concrete compressive strengths exceeding 40 MPa and the minimum requirement transverse reinforcement is not satisfied. Also, the ACI 318-08 approach [13] provides the constant efficiency factor when the minimum requirement reinforcement is satisfied. By means of,

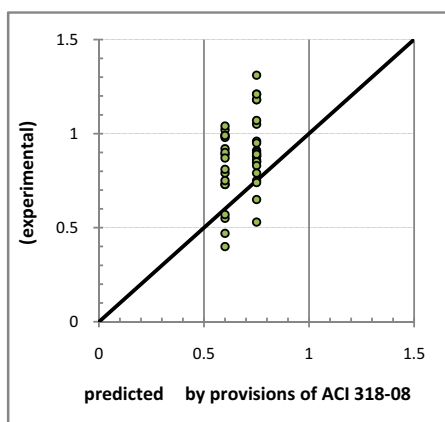




a. New model



b. CSA code



c. ACI 318-08

**Fig.16** Correlation between actual data and results of ACI 318-08, CSA and new model

the additional reinforcement cannot improve the efficiency factor. It needs for revision, because the experimental observation proved that, by increasing the amount of transverse reinforcement the effective strength of concrete

increases, especially in high-strength concrete.

b. The accurate prediction by provisions of CSA [12] needs to actual definition of  $\varepsilon_1$  the average principal tensile strain of concrete, this term can be measured in experimental studies, but many practicing users and designers have had difficulty in selecting an appropriate average tensile concrete strain. If the process could be simplified and the strain term eliminated, it would likely help design engineers.

## 9. Summery and Conclusion

1. In this paper a new model proposed for prediction of efficiency factor of concrete strength based on MCFT and mechanical behavior of cracked concrete.

2. In formulation of new model, the fully cracking assumed for concrete as the transverse reinforcement carries the transverse tensile force occurred in bottle-shaped strut.

3. The proposed model is more accurate in comparison with both ACI 318-08 and CSA approaches, consequently, it can be appropriate to develop to predict the shear strength of deep beams using the strut-and-tie method.

4. The magnitude of transverse tensile force is affected by slope of compression dispersion, and increases due to increasing the angle between diagonal strut and longitudinal axis of strut.

5. According to proposed model, the efficiency factor of concrete strength depends on specified strength of concrete as decreases by increasing the strength of concrete. It means that in RC structures constructed by high-strength concrete because of usual brittle failure, the principle role of transverse reinforcement is more sensitive than those by normal-strength concrete.

6. The ACI 318-08 provision proposed the most scattered results, as the predicted capacities are unsafe for under-reinforced specimens but conservative for over-reinforced those.

7. Because the accuracy of CSA provisions depends on definition an appropriate amount for average principal tensile strain of concrete, if the process could be simplified and the strain term eliminated, it would be more adequate and reliable to use in design works.

## References

- [1] Ritter, W., 1899, Die Bauweise Hennebique (The Hennebique System), Schweizerische Bauzeitung, Bd. XXXIII, No. 7, Zurich, Switzerland.
- [2] Mörsch, E., 1902, Der Eisenbetonbau, seine Theorie und Anwendung (Reinforced Concrete, Theory and Application), Stuttgart, Germany.
- [3] Marti, P. 1986, Staggered Shear Design of Simply Supported Concrete beams, ACI Journal, Vol. 83, No. 1, pp. 36-41
- [4] Schlaich, J., and Schäfer, K., 1991, Design and detailing of structural concrete using strut-and-tie models, The Structural Engineer, Vol. 69, No. 6, pp. 113-120.
- [5] Collins, M.P., and Mitchell, D., 1986, A Rational Approach to Shear Design The 1984 Canadian Code Provisions, ACI Journal, Vol. 83, No.6, pp 925-933.
- [6] Ramirez, J.A., and Breen, J.E., 1991, Evaluation of Modified Truss-Model Approach for Beams in Shear, ACI Structural Journal, Vol. 88, No. 5, pp. 562-571.

- [7] C. Y. Tang, and K. H. Tan., Interactive mechanical model for shear strength of deep beams, *JOURNAL OF STRUCTURAL ENGINEERING .ASCE*, Vol. 130, No. 10, 2004. pp.1534-1544.
- [8] Shyh-Jiann Hwang and Hung-Jen Lee, Strength prediction for discontinuity regions by softened strut-and-tie model, *JOURNAL OF STRUCTURAL ENGINEERING .ASCE*, Vol. 128, No. 12, 2002, pp.1519-1526.
- [9] A. Arabzadeh, A. R. Rahaei, R. Aghayari, 2009, A simple strut-and-tie model for prediction of ultimate shear strength of RC deep beams, *International journal of civil engineering*, IRAN, Vol. 7, No.3, pp. 141-154
- [10] Michael D. Brown, Cameron L. Sankovich, Oguzhan Bayrak, and James O. Jisra, Behavior and efficiency of bottle-shaped struts, *ACI STRUCTURAL JOURNAL*, Vol.103, No.3, 2006. pp. 348-355.
- [11] Michael D. Brown and Oguzhan Bayrak, Minimum Transverse Reinforcement for Bottle-Shaped Struts, *ACI STRUCTURAL JOURNAL*, Vol.103, No.6, 2006. pp. 813-821.
- [12] CSA Standard CAN3-A23.3-94, 1994, Design of Concrete Structures for Buildings with Explanatory Notes, Canadian Standards Association, Rexdale, Ontario.
- [13] ACI 318-08, 2008, Building Code Requirements for Structural Concrete and Commentary, American Concrete Institute, Farmington Hills, Michigan.
- [14] Schlaich, J. and Weischede, D., 1982, Detailing of Concrete Structures, Bulletin d'Information 150, Comité Euro-International du Béton, Paris, 163 pp. (in German)
- [15] A. Arabzadeh, R. Aghayari, A. R. Rahaei, 2009, Investigation of experimental and analytical shear strength of reinforced concrete deep beams, *International journal of civil engineering*, IRAN, Vol. 9, No.3, pp. 207-214
- [16] Vecchio, F.J. and Collins, M.P., 1986, The Modified Compression Field Theory for Reinforced Concrete Elements Subjected to Shear, *ACI Journal*, Vol. 83, No. 2, pp. 219-231